

Mental speed is associated with the shape irregularity of white matter MRI hyperintensity load

Catharina Lange^{1,2} · Per Suppa^{1,3} · Anja Mäurer⁴ · Kerstin Ritter⁵ · Uwe Pietrzyk^{2,6} · Elisabeth Steinhagen-Thiessen⁷ · Jochen B. Fiebach⁸ · Lothar Spies³ · Ralph Buchert¹

© Springer Science+Business Media New York 2016

Abstract Brain MRI white matter hyperintensities (WMHs) are common in elderly subjects. Their impact on cognition, however, appears highly variable. Complementing conventional scoring of WMH load (volume and location) by quantitative characterization of the shape irregularity of WMHs might improve the understanding of the relationship between WMH load and cognitive performance. Here we propose the “confluency sum score” (COSU) as a marker of the total shape irregularity of WMHs in the brain. The study included two independent patient samples: 87 cognitively impaired geriatric inpatients from a prospective neuroimaging study (iDSS) and 198 subjects from the National Alzheimer’s

Coordinating Center (NACC) database (132 with, 66 w/o cognitive impairment). After automatic segmentation and clustering of the WMHs on FLAIR (LST toolbox, SPM8), the confluency of the i -th contiguous WMH cluster was computed as $\text{confluency}_i = [1/(36\pi) \cdot \text{surface}_i^3 / \text{volume}_i^2]^{1/3} - 1$. The COSU was obtained by summing the confluency over all WMH clusters. COSU was tested for correlation with CERAD-plus subscores. Correlation analysis was restricted to subjects with at least moderate WMH load (≥ 13.5 ml; iDSS / NACC: $n = 52 / 80$). In the iDSS sample, among the 12 CERAD-plus subtests the trail making test A (TMT-A) was most strongly correlated with the COSU (Spearman $\rho = -0.345$, $p = 0.027$). TMT-A performance was not associated with total WMH volume ($\rho = 0.147$, $p = 0.358$). This finding was confirmed in the NACC sample ($\rho = -0.261$, $p = 0.023$ versus $\rho = -0.040$, $p = 0.732$). Cognitive performance in specific domains including mental speed and fluid abilities seems to be more strongly associated with the shape irregularity of white matter MRI hyperintensities than with their volume.

Electronic supplementary material The online version of this article (doi:10.1007/s11682-016-9647-x) contains supplementary material, which is available to authorized users.

✉ Ralph Buchert
ralph.buchert@charite.de

- ¹ Department of Nuclear Medicine, Charité – Universitätsmedizin Berlin, Berlin, Germany
- ² School of Mathematics and Natural Science, University of Wuppertal, Wuppertal, Germany
- ³ jung diagnostics GmbH, Hamburg, Germany
- ⁴ Evangelisches Geriatriezentrum Berlin, Berlin, Germany
- ⁵ Berlin Center for Advanced Neuroimaging, Bernstein Center for Computational Neuroscience, Charité – Universitätsmedizin Berlin, Berlin, Germany
- ⁶ Institute of Neuroscience and Medicine, Forschungszentrum Jülich, Jülich, Germany
- ⁷ Lipid Clinic at the Interdisciplinary Metabolism Center, Charité – Universitätsmedizin Berlin, Berlin, Germany
- ⁸ Center for Stroke Research Berlin, Charité – Universitätsmedizin Berlin, Berlin, Germany

Keywords White matter hyperintensities · MRI · FLAIR · Biomarker · Confluency · Cerebrovascular disease · CERAD

Background

MRI white matter hyperintensities (WMHs) are seen in virtually all elderly people, although to strongly variable extent. WMHs have been associated with the whole spectrum of cognitive decline / dysfunction, ranging from subjective cognitive decline over mild cognitive impairment to dementia (Chui and Ramirez-Gomez 2015; Chutinet and Rost 2014; Mortamais et al. 2014; H. J. Kim et al. 2015; Ye et al. 2015; Benedictus et al. 2015; Pantoni et al. 2015; Sun et al. 2016). However,

WMHs can be present also without any symptoms. Therefore, it is an important diagnostic step to decide whether WMH burden in a cognitively impaired patient is sufficiently severe to explain the impairment, or not. In the latter case, the patient might be referred to further diagnostic procedures in order to identify the underlying disease.

There is considerable evidence that WMH lesions can be associated with decline of cognitive performance in attention and executive function (DeBette and Markus 2010; Tate et al. 2008), visuoconstructional praxis, speed and motor control (Soriano-Raya et al. 2012), and working memory (Jokinen et al. 2009). However, the correlation between the severity of WMHs and cognitive performance has often found to be very weak (Sabri et al. 1999; Garde et al. 2000; R. Schmidt et al. 2002; Bracco et al. 1993). To some extent this might be explained by histopathological heterogeneity of WMHs (Gouw et al. 2011) and high variability of the severity of nerve fiber damage within WMH lesions (Galluzzi et al. 2008). Another source of variability most likely is the varying involvement of different white matter fasciculi.

Total volume and location of WMHs are the most straightforward parameters for characterizing the brain's WMH load. However, quantitative measures and visual scores of WMH load that are mainly based on the volume and location of WMHs might be not sufficient to fully characterize the severity of WMH load. This, too, might have contributed to the relative inconsistency of neuroimaging findings regarding the impact of WMH on cognitive performance.

There is increasing evidence that the shape of WMH lesions provides additional information that is independent of the lesion volume (Gouw et al. 2011; Chui and Ramirez-Gomez 2015). Smooth lesions surrounding the inner ventricles (periventricular WMHs, “small caps”) or spherical WMH lesions are thought to have less impact on cognition than more irregular confluent WMH lesions (Scarpelli et al. 1994; Chimowitz et al. 1992; Fazekas et al. 1993; K. W. Kim et al. 2008). Furthermore, visual scores used for the assessment of WMH load in clinical routine patient care (Wahlund et al. 2001; Fazekas et al. 1987; Scheltens et al. 1993) show rather large variability not only between raters (inter-rater variability), but also when the same rater repeats the scoring of the same image (intra-rater variability) (van den Heuvel et al. 2006; Prins et al. 2004; Kapeller et al. 2003). This variability might also mask the association between WMH load and cognitive performance.

Thus, there is a need for clinically useful measures of WMH load beyond lesion volume and location that can be obtained with high inter- and intra-rater stability. Here we propose the confluency sum score (COSU) for quantitative characterization of the total shape irregularity of the WMH load. The COSU is computed automatically based on automatic segmentation of WMH lesions on FLAIR images and, thus, is fully rater-independent.

Methods

Patients

This study included two independent patient samples. The first sample was drawn from the prospective observational neuroimaging study “Comparison and integration of modalities in the early and differential diagnosis of dementing disorders in hospitalized geriatric patients: a prediction study” (WHO Trials Registry DRKS00005041, acronym: iDSS). The iDSS study made no a priori hypotheses with respect to the COSU so that the analyses presented here are retrospective in nature. Therefore, a second patient sample was assembled from the National Alzheimer's Coordinating Center (NACC) database (<https://www.alz.washington.edu/>) in order to provide an independent test of the results obtained in the iDSS sample.

iDSS sample

The iDSS study is an ongoing study on the add-on diagnostic value of neuroimaging in newly diagnosed cognitive impairment in geriatric inpatients hospitalized due to acute indications. It includes patients with newly manifested cognitive impairment during the current hospital stay and a clinical suspicion of neurodegenerative etiology. For the analyses presented here, we included all subjects who successfully completed structural MRI (i.e. T1-weighted MPRAGE and T2-weighted FLAIR) and for whom an etiological diagnosis of their cognitive impairment by an interdisciplinary team of academic experts was available ($n = 87$). The etiological diagnoses included non-neurodegenerative etiology ($n = 15$), Alzheimer's disease (AD, $n = 17$), cerebrovascular disease (CVD, $n = 23$), mixed disease (MD, defined as concurrence of AD and CVD, $n = 25$), and neurodegenerative etiology other than AD ($n = 7$). Subject characteristics are summarized in Online Resource 1.

MRI of the brain, including 3-dimensional T1-weighted MPRAGE (1x1x1 mm³) and T2-weighted FLAIR (in-plane: 1.2 mm, slice thickness: 2.5 mm), had been performed with the same 3 Tesla MR scanner (Siemens TimTrio) in all patients. MR examination had been performed between 7 days before to 9 days after neuropsychological testing (median delay of 1 day).

NACC sample

Since the proposed COSU marker is expected to be most useful in patients with at least moderate WMH load, the NACC database was first searched for patients with suspected vascular dementia (VaD) using the following eligibility criteria: (i) primary or contributing diagnosis of probable or

possible VaD based on NINDS-AIREN criteria (Roman et al. 1993) that was stable over all follow-up visits, and (ii) availability of high-resolution T1-weighted MPRAGE and T2-weighted FLAIR. This resulted in the inclusion of 66 patients (referred to NACC-VaD patients). MR imaging had been performed before or after neuropsychological testing (median delay of 7 days, range: 1727 days before to 2543 days after the visit).

Then the NACC database was searched for AD patients and cognitively normal controls (NC). The following criteria were applied: AD patients (NACC-AD): primary diagnosis of probable AD based on NINCDS/ADRDA criteria (McKhann et al. 1984) that was stable over all follow-up visits (at least one); NC subjects (NACC-NC): (i) normal cognition that was stable over all follow-up visits (at least three years), (ii) no major neurological or psychiatric disease, no CNS neoplasm. For both, NACC-AD and NACC-NC, the delay between MR acquisition and neuropsychological testing was restricted to a maximum of 100 days. From the NACC-AD subjects identified by the search, 66 subjects were selected using a “match by subject” approach to match the NACC-VaD group with respect to age and sex. A NACC-NC cohort of 66 subjects was generated analogously. Subject characteristics are summarized in Online Resource 2.

NACC MRI data used here had been acquired at six different centers using eight different scanner models of three different manufacturers. Median resolution of the 3-dimensional T1-weighted MPRAGE was $1.0 \times 1.0 \times 1.2 \text{ mm}^3$, median in-plane resolution and slice thickness of the T2-weighted FLAIR were 1.0 mm and 3.0 mm, respectively.

Automatic segmentation of white matter hyperintensities

For automatic segmentation of WMHs, the freely available lesion segmentation toolbox (LST) under the statistical parametric mapping software package (version SPM8) was used with default parameter settings (“kappa” = 0.30, “binary” = 0.50, lesion growth algorithm, LGA) (P. Schmidt et al. 2012; Frackowiak et al. 2004). The LST provides a binarized WMH map.

Confluency sum score

The 3-dimensional WMH map generated by the LST was clustered into separate WMH lesions using the SPM8 routine `spm_bwlabel` which labels connected components on the basis of a connectivity criterion to be specified. The “surface” connectivity criterion was used here, i.e. two WMH voxels were considered as connected if they had one surface in common (a common edge or a common vertex was not sufficient).

Then the confluency of the i -th WMH lesion was calculated according to the following definition

$$\text{confluency}_i = \sqrt[3]{\frac{1}{36\pi} \frac{\text{surface}_i^3}{\text{volume}_i^2}} - 1 \quad (1)$$

The formula on the right-hand side (or a very similar one) has previously been used in geology for scale invariant definition of the “sphericity” of quartz particles (Wadell 1935). In medicine it has been used to define the “asphericity” of the metabolically active part of a tumor in whole body positron emission tomography with the glucose analog F-18-fluorodeoxyglucose (Apostolova et al. 2014a; Apostolova et al. 2014b; Hofheinz et al. 2014).

The surface (surface_i) and the volume (volume_i) of the i -th WMH lesion were obtained by counting voxels in the binary WMH map which is very efficient computationally. The confluency as defined in Eq. 1 is scaled such that the confluency is 0 for a sphere and larger than 0 for all other shapes.

In practice, the computation of the confluency is limited by the fact that MR images are composed of voxels with uniform signal intensity. Thus, there is no perfect sphere in MR images, but only “edgy” approximations. Computer simulations showed that the resulting error in the confluency can be neglected for spheres composed of at least 100 voxels (results not shown).

In order to provide one single quantitative measure of total shape irregularity of all WMHs throughout the whole brain, the confluency was summed over all WMH lesions composed of ≥ 100 voxels to obtain the confluency sum score (COSU):

$$\text{COSU} = \sum_i^N \text{confluency}_i \quad (2)$$

where N is the total number of lesions in the WMH map composed of ≥ 100 voxels. The COSU of any WMH pattern consisting of two or more spherical lesions is zero. The COSU becomes larger than zero when two or more of these spherical lesions merge (confluence) to form a non-spherical lesion. The COSU usually increases with increasing number of spherical lesions that merge, as the shape irregularity (confluency according to Eq. 1) of the resulting lesion tends to increase. The COSU also increases when a single lesion becomes more irregularly shaped during its growth.

The total WMH volume was computed as

$$\text{total WMH volume} = \sum_i^N V_i \quad (3)$$

where V_i is the volume of the i -th WMH lesion (obtained by multiplying the number of voxels in the lesion by the voxel volume). N is the total number of WMH lesions with ≥ 100 voxels, i.e. the total WMH volume included the same WMH lesions as the COSU (Eq. 2). This was to avoid any bias in

favor of one or the other measure (COSU or total WMH volume) that might affect their comparison with respect to their association with cognitive performance.

Association between the confluency sum score and cognitive performance

In order to detect possible associations between the COSU (and / or the total WMH volume) with the performance in various cognitive domains, the COSU (and total WMH volume) in the iDSS sample was tested for correlation with each of 12 subscores of the test battery of the Consortium to Establish a Registry for Alzheimer's Disease (CERAD, CERAD-plus version) (Morris et al. 1988). The CERAD test battery provides tests of verbal fluency (by naming animals), an abbreviated version of the Boston naming test (15 items), mini-mental state examination (MMSE), word list learning / recall / recognition test, constructional praxis, and recall of constructional praxis. In CERAD-plus, the trail making test A (TMT-A), trail making test B (TMT-B) and a phonematic fluency test ("s-words") are included. All subscores were transformed to z-scores corrected for age, sex and education using the Excel spreadsheet (<https://www.memoryclinic.ch/de/main-navigation/neuropsychologen/cerad-plus/auswertungprogramme/cerad-plus-10-excel/>) based on two normative samples for the German CERAD-plus version ($n = 1100$ for the standard tests, $n = 604$ for the plus tests) (Ehrensperger et al. 2010). In the NACC sample five CERAD subscores were available (animals, Boston, MMSE, TMT-A and -B). These were transformed to age, sex and education corrected z-scores using the Excel spreadsheet provided as online resource by Shirk and colleagues (Shirk et al. 2011) based on 3268 cognitively normal older subjects of the NACC Uniform Data Set. The non-parametric Spearman test was used for bivariate correlation analyses in order to avoid spurious correlations that might be caused by outliers when using the parametric Pearson correlation test.

The bivariate correlation analyses revealed a significant correlation of the COSU (but not total WMH volume) with the performance in TMT-A (s. Results section). In order to test the specificity of this finding, partial correlation analyses correcting for overall cognitive performance (as measured by the MMSE) were performed. Furthermore, correlation was controlled for the etiology, i.e. with neurodegenerative disease (iDSS sample: AD, MD and 'neurodegenerative diseases other than AD', NACC sample: AD) versus without neurodegenerative disease (iDSS sample: CVD and 'other non-neurodegenerative diseases', NACC sample: VaD and NC), and for ApoE genotype (number of E4 alleles).

In order to assess the potential impact of considerable interindividual variability in the interval between imaging and cognitive testing and of heterogeneity of MR scanners and

MR acquisition protocols in the NACC sample, additional partial correlation analyses were performed in the NACC sample correcting (i) for the time delay between MR acquisition and cognitive testing, or (ii) for the magnetic field strength of the MR scanner (1.5 versus 3 T) or (iii) for the voxel volume in the FLAIR image.

Since WMH load might be considered the underlying cause of cognitive impairment only if it is "sufficiently" severe, only subjects with a total WMH load of ≥ 13.5 ml were included in the correlation analyses. This threshold had been determined in the iDSS cohort, in which visual scoring of the severity of WMH load by an experienced neuro-radiologist as either "normal for age" or "more than normal for age" was available. Receiver operating characteristic (ROC) analysis of the total WMH volume for differentiation between "normal for age" and "more than normal for age" WMH load revealed an area under the ROC curve of 0.944. The Youden criterion resulted in a total volume of 13.5 ml as optimal cut-off (Youden 1950).

Results

WMH segmentation

Fully automatic segmentation of WMHs worked properly in 86 of the 87 iDSS subjects and in 193 of the 198 NACC subjects according to visual inspection of the binary WMH map overlaid as contour to the corresponding FLAIR (Fig. 1).

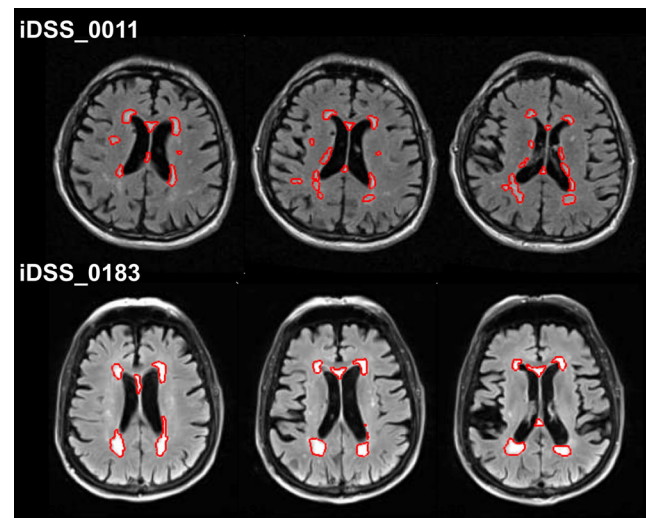


Fig. 1 Two iDSS subjects with similar total WMH volume (iDSS_0011: 18.3 ml and iDSS_0183: 18.6 ml), but different confluency sum score (COSU) of the WMHs (21.9 and 8.8, respectively). The performance in the trail making test A was more strongly impaired in the subject with the larger COSU (z-score -2.4 and -1.0 , respectively). The red contour represents the automatically segmented white matter hyperintensities overlaid to the individual FLAIR image in native space. Three consecutive slices at the level of the inner ventricles are displayed for each subject

In the remaining 6 subjects, automatic segmentation resulted in strong underestimation ($n = 5$) or strong overestimation of the WMH lesion load ($n = 1$). These subjects were excluded from further analyses.

The total volume of WMH lesions ranged from 0.24 ml to 74.92 ml in the iDSS sample and from 0.00 ml to 74.37 ml in the NACC sample. Detailed results stratified according to etiological subgroups are given in Online Resources 1, 2.

Total processing time for WMH segmentation strongly depended on the individual lesion load. Average time on a standard PC was 20 min.

Confluency sum score

The COSU ranged from 0.89 to 26.44 in the iDSS sample and from 0.00 to 18.20 in the NACC sample. Detailed results stratified according to etiological subgroups are given in Online Resources 1, 2.

Association between the confluency sum score and cognitive performance

The tests for association between the COSU (or total WMH load) with the CERAD-plus subscores included all subjects in whom automatic WMH segmentation had worked properly and resulted in total WMH volume ≥ 13.5 ml (s. subsection “Association between the confluency sum score and cognitive performance” in Methods): 52 iDSS subjects and 80 NACC subjects. A detailed description of these subjects is given in Tables 1 and 2.

The results of the correlation analyses are summarized in Table 3. In the iDSS sample, among all CERAD-plus subscores the TMT-A z-score showed the strongest correlation with the COSU (Spearman correlation coefficient $\rho = -0.345$, $p = 0.027$; Fig. 2a), but it was not correlated with the total WMH volume ($\rho = 0.147$, $p = 0.358$; Fig. 2b). The two iDSS subjects in Fig. 1 present with very similar total WMH volume (18.3 versus 18.6 ml) but different COSU (21.9 versus 8.8). The subject with the larger COSU performed worse in the TMT-A (z-score -2.4 versus -1.0).

The correlation pattern of TMT-A performance with WMH load, i.e. moderate negative correlation with the COSU and no correlation with total volume, was confirmed in the NACC sample ($\rho = -0.261$, $p = 0.023$, versus $\rho = -0.040$, $p = 0.732$; Table 3, Fig. 2 c, d). In the NACC sample, TMT-B, animals and MMSE also showed a significant correlation with the COSU (Table 3).

The correlation between the COSU and TMT-A performance in the iDSS sample did not reach the significance level after Bonferroni-Holm correction for multiple testing. However, in the NACC sample, the correlations between the COSU and the animals subtest and TMT-B performance remained statistically significant at the 5 % level after

Bonferroni-Holm correction (they would also survive the more restrictive conventional Bonferroni adjustment). The correlation between the COSU and TMT-A performance only slightly missed the Bonferroni-Holm corrected significance level.

Further confirmation of the association between TMT performance and the COSU was provided by the partial correlation analyses that removed the effect of overall cognitive performance (MMSE) or the effect of neurodegeneration or the effect of ApoE genotype (Online Resource 3). Correction for the time interval between imaging and cognitive testing or MR field strength or FLAIR voxel volume in the NACC sample did also not affect the main finding: the negative correlation between TMT performance and the COSU remained statistically significant in all cases (Online Resources 4).

In the patients with low WMH burden (WMH volume < 13.5 ml), there was no correlation (according to the Spearman test) of the COSU (or total WMH volume) with any of the CERAD-plus subscore, neither in the iDSS sample ($n = 34$) nor in the NACC sample ($n = 113$).

Discussion

The present study proposes the confluency sum score (COSU) as novel marker of the total shape irregularity of brain WMHs. The COSU was defined in such a way that it is independent of the volume of WMHs (scale invariant). The COSU was tested for correlation with cognitive performance in two patient samples.

In the iDSS sample, among the 12 subtests of the CERAD-plus test battery the trail making test A (TMT-A) was most strongly correlated with the COSU. However, TMT-A performance was not significantly correlated with the total WMH volume. This finding was confirmed in an independent sample of subjects from the NACC database. In the NACC sample, the trail making test B (TMT-B), too, was significantly correlated with the COSU, in line with the general expectation that subjects with impaired TMT-A performance should also show impaired TMT-B performance. The fact that there was no significant correlation between TMT-B performance and the COSU in the iDSS sample might be explained by the low number of iDSS subjects for this specific test due to the particularly high fraction of missing TMT-B z-scores (Table 1). This was most likely due to the overall lower cognitive performance of the iDSS subjects compared to the NACC subjects which prevented many iDSS subjects from successfully completing the TMT-B so that no z-score could be assigned (MMSE z-score $= -3.53 \pm 1.58$ versus -2.86 ± 3.62 , in iDSS subjects and NACC subjects, respectively, $p = 0.031$, Online Resources 1, 2). The correlation between TMT-A performance and the COSU remained statistically significant when the effect of overall cognitive performance (MMSE) was

Table 1 Characteristics of the iDSS subsample used for the correlation analyses (total WMH volume ≥ 13.5 ml). Numbers are given as mean \pm standard deviation [range] (deviant sample size).

Characteristic	Non-neurodegenerative (<i>n</i> = 5)	AD (<i>n</i> = 3)	CVD (<i>n</i> = 18)	MD (<i>n</i> = 24)	Other neurodegenerative than AD (<i>n</i> = 2)	all (<i>n</i> = 52)	<i>p</i> - value*
Age [years]	84.60 \pm 4.34	76.67 \pm 0.58	81.78 \pm 5.84	83.33 \pm 4.79	81.00 \pm 2.83	82.44 \pm 5.14	.349
Sex [females]	4 / 80.0 %	0 / 0.0 %	11 / 61.1 %	16 / 66.7 %	2 / 100.0 %	33 / 63.5 %	.121
Education [years]	10.20 \pm 2.28	17.00 \pm 1.00	12.69 \pm 4.20	12.29 \pm 3.41	9.50 \pm 2.12	12.39 \pm 3.71	.733
<i>CERAD-plus</i> [<i>z</i> -scores]							
Animals	-0.56 \pm 1.03	-2.37 \pm 0.85	-1.62 \pm 0.83	-1.70 \pm 0.95	-1.95 \pm 1.91	-1.61 \pm 0.98	.783
Boston	-0.08 \pm 1.82	-0.37 \pm 1.50	-0.56 \pm 1.14	-0.31 \pm 1.28 (<i>n</i> = 23)	-0.95 \pm 0.21	-0.40 \pm 1.25 (<i>n</i> = 51)	.516
MMSE	-2.94 \pm 2.33	-3.43 \pm 1.98	-3.06 \pm 1.78	-3.95 \pm 1.40	-3.50 \pm 1.27	-3.50 \pm 1.66	.075
Learning word list	-1.70 \pm 1.02	-2.57 \pm 2.22	-2.36 \pm 1.00	-2.44 \pm 1.56	-2.35 \pm 2.33	-2.35 \pm 1.36	.840
Copy figures	-1.42 \pm 0.89	-1.10 \pm 1.66	-1.10 \pm 1.29	-1.57 \pm 1.21 (<i>n</i> = 23)	-1.85 \pm 0.71	-1.38 \pm 1.20 (<i>n</i> = 51)	.234
Recall word list	-1.86 \pm 0.82	-2.23 \pm 1.44	-1.68 \pm 1.06	-2.26 \pm 1.19 (<i>n</i> = 23)	-1.65 \pm 1.20	-1.99 \pm 1.12 (<i>n</i> = 51)	.116
Word list intrusions	-1.24 \pm 0.43	-0.43 \pm 1.12	-0.95 \pm 1.55	-1.17 \pm 1.23	-0.40 \pm 1.98	-1.03 \pm 1.30	.617
Recognition word list	-1.14 \pm 1.13	0.00 \pm 1.73	-0.86 \pm 1.60	-0.90 \pm 1.52 (<i>n</i> = 23)	-2.00 \pm 0.14	-0.90 \pm 1.49 (<i>n</i> = 51)	.937
Recall figures	-1.24 \pm 1.09	-1.03 \pm 1.63	-1.74 \pm 0.96	-2.00 \pm 0.92 (<i>n</i> = 23)	-1.90 \pm 1.27	-1.78 \pm 1.00 (<i>n</i> = 51)	.375
TMT-A	-1.38 \pm 1.11 (<i>n</i> = 4)	-3.25 \pm 0.21 (<i>n</i> = 2)	-1.23 \pm 0.86 (<i>n</i> = 16)	-1.69 \pm 0.80 (<i>n</i> = 17)	-1.15 \pm 1.48	-1.53 \pm 0.94 (<i>n</i> = 41)	.119
TMT-B	-1.40 \pm 0.71 (<i>n</i> = 2)	-1.80 (<i>n</i> = 1)	-1.24 \pm 1.29 (<i>n</i> = 5)	-1.65 \pm 0.79 (<i>n</i> = 4)	-1.30 (<i>n</i> = 1)	-1.44 \pm 0.89 (<i>n</i> = 13)	.596
S-word list	-0.26 \pm 1.53	-1.80 \pm 1.81	-1.39 \pm 1.15	-1.41 \pm 0.99 (<i>n</i> = 23)	-1.75 \pm 0.35	-1.33 \pm 1.16 (<i>n</i> = 51)	.953
<i>WMH</i>							
Total volume [ml]	18.52 \pm 2.65 [14.61–21.58]	22.02 \pm 5.04 [16.47–26.31]	41.07 \pm 17.73 [13.97–74.92]	35.40 \pm 15.45 [14.87–72.98]	18.57 \pm 1.11 [17.79–19.36]	34.32 \pm 16.55 [13.97–74.92]	.276
COSU	13.28 \pm 5.27 [8.13–21.88]	18.96 \pm 5.86 [14.13–25.48]	12.25 \pm 2.58 [7.73–19.90]	13.55 \pm 4.05 [6.69–26.44]	7.97 \pm 1.81 [6.69–9.25]	13.17 \pm 4.08 [6.69–26.44]	.241

AD Alzheimer's disease, *COSU* confluency sum score, *CVD* cerebrovascular disease, *MD* mixed etiology, *MMSE* mini-mental state examination, *TMT* trail making test, *WMH* white matter hyperintensities

*t-test comparison of numerical characteristics (all except sex) between 'CVD' and 'MD'. The chi square test was used to compare the distribution of sex between these two groups. The other three diagnostic groups ('non-neurodegenerative', 'AD', 'other neurodegenerative than AD') were not included in the comparisons because of their small sample size.

Table 2 Characteristics of the NACC subsample used for the correlation analyses (total WMH volume ≥ 13.5 ml). Numbers are given as mean \pm standard deviation [range] (deviant sample size).

Characteristic	AD (n = 29)	VaD (n = 33)	NC (n = 18)	all (n = 80)	p-value* (ANOVA)
Age [years]	80.86 \pm 6.15	83.92 \pm 5.46	82.98 \pm 4.30	82.60 \pm 5.60	.094
Sex [females]	13 / 44.8 %	18 / 54.5 %	12 / 66.7 %	43 / 53.8 %	.342
Education [years]	14.62 \pm 2.83	14.09 \pm 3.69	16.17 \pm 2.38	14.75 \pm 3.20	.081
<i>CERAD-plus [z-scores]</i>					
Animals	-1.61 \pm 0.75	-1.23 \pm 0.82	-0.25 \pm 0.61	-1.15 \pm 0.90	.000 ^{b,c}
Boston	-2.90 \pm 2.10	-2.15 \pm 1.61 (n = 31)	-0.34 \pm 0.78	-2.01 \pm 1.92 (n = 78)	.000 ^{b,c}
MMSE	-5.88 \pm 3.05	-3.78 \pm 3.57 (n = 32)	0.42 \pm 1.08	-3.59 \pm 3.78 (n = 79)	.000 ^{a,b,c}
TMT-A	-1.89 \pm 2.94	-2.41 \pm 2.98 (n = 29)	0.20 \pm 0.80	-1.59 \pm 2.78 (n = 76)	.004 ^{b,c}
TMT-B	-3.41 \pm 1.60 (n = 28)	-2.38 \pm 1.59 (n = 25)	-0.18 \pm 0.84	-2.23 \pm 1.92 (n = 71)	.000 ^{b,c}
<i>WMH</i>					
Total volume [ml]	29.77 \pm 14.63 [14.30–69.87]	32.63 \pm 15.55 [13.74–74.37]	27.89 \pm 11.24 [13.63–49.09]	30.53 \pm 14.30 [13.63–74.37]	.502
COSU	11.20 \pm 2.85 [7.74 \pm 17.93]	9.41 \pm 2.89 [4.71–17.54]	9.08 \pm 2.29 [6.22–13.44]	9.98 \pm 2.87 [4.71–17.93]	.014 ^{a,b}

AD Alzheimer's disease, COSU confluency sum score, MMSE mini-mental state examination, NC normal control, TMT trail making test, VaD vascular dementia, WMH white matter hyperintensities

^a Post-hoc analysis: significant group difference between 'AD' and 'VaD'

^b Post-hoc analysis: significant group difference between 'AD' and 'NC'

^c Post-hoc analysis: significant group difference between 'VaD' and 'NC'

*Comparison of numerical characteristics (all except sex) between the three groups was performed by one-way ANOVA. In case of a significant between groups effect, post hoc multiple comparisons were performed using either Scheffe's test (assuming equal variance) or Tamhane's test (unequal variance), depending on the result of Levene's test for homogeneity of variance. The chi-square test was used to compare the distribution of sex between the three groups. In case of a significant between groups effect, the chi square test was applied to all possible pairs of two groups. A significance level of $\alpha = 0.05$ was assumed for between all groups tests as well as for post hoc tests

removed (Online Resource 3). Furthermore, the association between COSU and TMT-A performance was independent of the presence (versus absence) of a neurodegenerative disease, it was also independent of ApoE genotype (Online Resource 3).

When the analyses were performed separately in the different diagnostic subgroups of the NACC sample, the correlation between the COSU and TMT performance did not reach the level of statistical significance (results not shown). Possible

Table 3 Results of the Spearman test for correlation between the performance in the CERAD-plus subtests (z-scores) and either the COSU or the total WMH volume. The value given is the Spearman correlation coefficient rho. Statistical significance is indicated by an asterisk (*p-value ≤ 0.05 ; **p-value ≤ 0.01)

CERAD-plus [z-scores]	iDSS		NACC	
	Total volume [ml]	COSU	Total volume [ml]	COSU
Animals	-.101	.072	-.222*	-.329**
Boston	-.123	.178	-.174	-.114
MMSE	-.183	-.045	-.054	-.250*
Learning word list	-.166	.033	N/A	N/A
Copy figures	-.069	-.032	N/A	N/A
Recall word list	-.093	-.040	N/A	N/A
Wordlist intrusions	.117	.255	N/A	N/A
Recognition word list	.223	.130	N/A	N/A
Recall figures	-.266	.057	N/A	N/A
TMT-A	.147	-.345*	-.040	-.261*
TMT-B	-.019	.171	-.021	-.335**
S-word list	-.061	.080	N/A	N/A

COSU confluency sum score, MMSE mini-mental state examination, N/A not available, TMT trail making test, WMH white matter hyperintensities

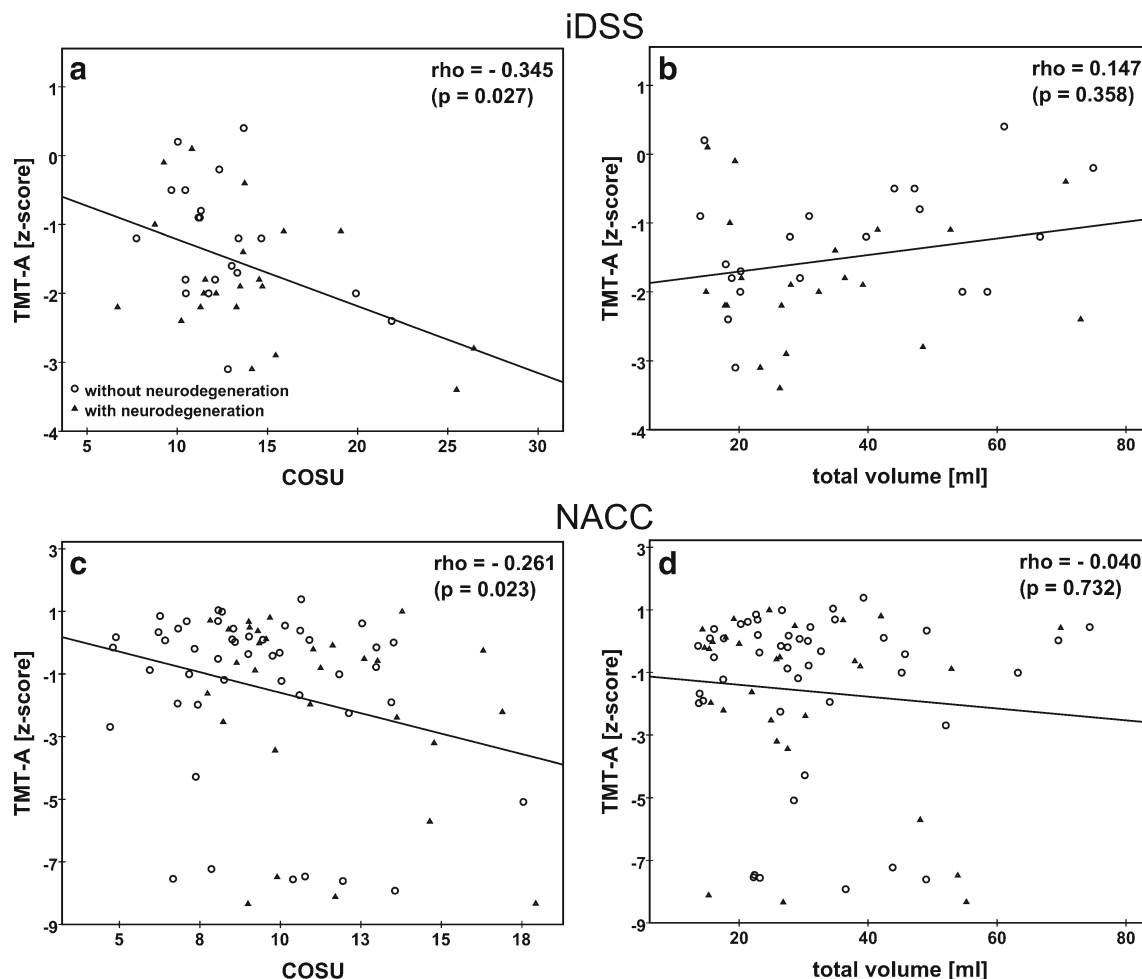


Fig. 2 Association between the performance in the trail making test A (z-score) and the WMH confluency sum score (COSU) or the total WMH volume (ml) in the iDSS and in the NACC sample. Different symbols are used for subjects with neurodegenerative disease (iDSS sample: AD, MD and ‘neurodegenerative diseases other than AD’, NACC sample: AD) and subjects without neurodegenerative disease (iDSS sample: CVD and ‘other non-neurodegenerative diseases’, NACC sample: VaD and NC). The Spearman correlation coefficient ρ and its p -value is

displayed in each panel. The line represents the result of linear regression. The NACC sample includes 9 subjects who completed the TMT-A test in more than 150 s which, however, is the time limit for this test (Weintraub et al. 2009). For the computation of z-scores, the completion time was set to 150 s in these subjects. Repeat Spearman analysis in the NACC sample without these 9 subjects resulted in $\rho = -0.239$ ($p = 0.052$) and $\rho = 0.049$ ($p = 0.691$) for the correlation between TMT-A performance and the COSU or total volume, respectively.

explanations include reduced statistical power by the rather small sample size of these subgroups (VaD: $n = 33$, AD: $n = 29$, NC: $n = 18$).

The total WMH volume (unit ml) is not scale invariant, in contrast to the COSU (unitless). This means that varying brain size might obscure possible associations of cognitive performance with total WMH volume (but not with COSU). In order to test this, total WMH volume was scaled to the individual total intracranial volume obtained by the reverse brain mask method as described in (Keihaninejad et al. 2010). Correlation analyses were repeated with the scaled total WMH volume (in %). TMT-A performance was not correlated with the scaled total WMH volume, neither in the iDSS sample ($\rho = 0.199$, $p = 0.211$) nor in the NACC sample ($\rho = -0.105$, $p = 0.365$).

The COSU correlates with the total number of WMH clusters, as is to be expected from its definition. Therefore, it might

be worth noting that the association between TMT-A performance and the total number of WMH clusters did not fully reach the level of statistical significance ($\rho = -0.292$, $p = 0.064$, and $\rho = -0.202$, $p = 0.080$, for iDSS and NACC, respectively), in contrast to the COSU. This suggests that the COSU provides useful information not only beyond the total WMH volume but also beyond the total number of WMH lesions over which the total volume is spread.

The 13.5 ml total WMH threshold for subjects to be included in the tests of imaging-cognition associations was derived in the iDSS sample, which might have introduced some circularity. However, this most likely is only a minor limitation, since additional information (visual scoring of the severity of WMH load by an experienced neuro-radiologist as either ‘normal for age’ or ‘more than normal for age’) was used for fixing the threshold, that is, the threshold was not

fixed by optimizing the correlation between the COSU and CERAD subscores. In addition, there is no risk of circularity by this threshold in the NACC sample.

TMT performance is known to be a sensitive marker of organic brain damage including diffuse cerebrovascular disease (Reitan 1958). Cognitive domains most strongly involved in TMT performance are mental speed and fluid cognitive abilities (Salthouse 2011). Thus, the present findings suggest that mental speed and fluid cognitive abilities are more strongly associated with the COSU than with the total WMH volume. The pathophysiology underlying this finding is unclear. The mechanisms by which WMH lesions affect cognitive function most likely include local damage of nerve fibers. Thus, the stronger association of processing speed and fluid cognitive abilities with COSU than with total WMH volume might be related to the fact that the larger WMH surface associated with larger COSU at the same total WMH volume allows interference with more white matter fasciculi (in an extreme case, a thin WMH “plate”, small volume but large confluency, might interfere with all fasciculi connecting posterior and anterior brain or left and right hemisphere). This hypothesis might be tested using diffusion tensor tractography (O’Sullivan 2010) or resting state functional MRI to assess functional connectivity as a function of COSU and total WMH volume.

The specific association pattern of CERAD-plus subtests with the COSU, most pronounced in the TMTs, which was quite different from the association pattern with the total WMH volume, most pronounced in the listing animals test (verbal fluency), suggests that the COSU provides additional information independent of the total WMH volume. Thus, combining total WMH volume and COSU in multivariate models might explain more variance in cognitive function than WMH volume alone and, therefore, could be useful in the diagnostic workup of elderly people with cognitive impairment and WMHs in MRI. It might help to avoid overdiagnosing vascular dementia by improved differentiation between “significant” and “non-significant” WMH patterns (Niemantsverdriet et al. 2015).

Finally, in order to ensure the COSU to be rater-independent and fully reproducible, it should be computed automatically, which requires automatic segmentation of the WMHs. In the present study the lesion segmentation toolbox (LST) was used for this purpose. Although this toolbox was proposed for segmentation of demyelinating lesions in subjects with multiple sclerosis (Valverde et al. 2015; Muhlau et al. 2013; Mazerolle et al. 2013), the algorithm provided reliable segmentation of WMH in both samples of elderly subjects included in the present study. The LST failed according to visual inspection in only 6 of 285 cases (2.1 %). This is particularly remarkable as the multi-center MRI data of the NACC database was quite heterogeneous with respect to general image quality and contrast

(no subject was excluded based on technical constraints such as poor MR image quality). The fact that the LST worked properly under these challenging conditions demonstrates the robustness of the method, which is an important prerequisite for use in everyday clinical patient care.

Conclusion

Cognitive performance in specific domains including mental speed and fluid abilities seems to be more strongly associated with the COSU than with the total WMH volume. This suggests that combining total WMH volume and COSU in multivariate models might explain more variance in cognitive function than WMH volume alone and, therefore, could be useful in the diagnostic workup of elderly people with cognitive impairment and WMHs in MRI.

Acknowledgments The NACC database is funded by NIA/NIH Grant U01 AG016976. NACC data are contributed by the NIA funded ADCs: P30 AG019610 (PI Eric Reiman, MD), P30 AG013846 (PI Neil Kowall, MD), P50 AG008702 (PI Scott Small, MD), P50 AG025688 (PI Allan Levey, MD, PhD), P50 AG047266 (PI Todd Golde, MD, PhD), P30 AG010133 (PI Andrew Saykin, PsyD), P50 AG005146 (PI Marilyn Albert, PhD), P50 AG005134 (PI Bradley Hyman, MD, PhD), P50 AG016574 (PI Ronald Petersen, MD, PhD), P50 AG005138 (PI Mary Sano, PhD), P30 AG008051 (PI Steven Ferris, PhD), P30 AG013854 (PI M. Marsel Mesulam, MD), P30 AG008017 (PI Jeffrey Kaye, MD), P30 AG010161 (PI David Bennett, MD), P50 AG047366 (PI Victor Henderson, MD, MS), P30 AG010129 (PI Charles DeCarli, MD), P50 AG016573 (PI Frank LaFerla, PhD), P50 AG016570 (PI Marie-Francoise Chesselet, MD, PhD), P50 AG005131 (PI Douglas Galasko, MD), P50 AG023501 (PI Bruce Miller, MD), P30 AG035982 (PI Russell Swerdlow, MD), P30 AG028383 (PI Linda Van Eldik, PhD), P30 AG010124 (PI John Trojanowski, MD, PhD), P50 AG005133 (PI Oscar Lopez, MD), P50 AG005142 (PI Helena Chui, MD), P30 AG012300 (PI Roger Rosenberg, MD), P50 AG005136 (PI Thomas Montine, MD, PhD), P50 AG033514 (PI Sanjay Asthana, MD, FRCP), P50 AG005681 (PI John Morris, MD), and P50 AG047270 (PI Stephen Strittmatter, MD, PhD).

Compliance with ethical standards

Funding This work was supported by the Regional Development Fund of the European Union (10153407, 10153971, 10153458, 10153460, 10153461, 10153462, 10153463).

Conflict of interest P.S. and L.S. are employees of jung diagnostics GmbH. The remaining authors declare that they have no conflict of interest.

Ethical approval All procedures performed in studies involving human participants were in accordance with the ethical standards of the institutional and/or national research committee and with the 1964 Helsinki declaration and its later amendments or comparable ethical standards.

Informed consent Informed consent was obtained from all individual participants included in the study.

References

- Apostolova, I., Rogasch, J., Buchert, R., Wertzel, H., Achenbach, H. J., Schreiber, J., et al. (2014a). Quantitative assessment of the asphericity of pretherapeutic FDG uptake as an independent predictor of outcome in NSCLC. *BMC Cancer*, *14*, 896. doi:10.1186/1471-2407-14-896.
- Apostolova, I., Steffen, I. G., Wedel, F., Lougovski, A., Marnitz, S., Derlin, T., et al. (2014b). Asphericity of pretherapeutic tumour FDG uptake provides independent prognostic value in head-and-neck cancer. *European Radiology*, *24*(9), 2077–2087. doi:10.1007/s00330-014-3269-8.
- Benedictus, M. R., van Harten, A. C., Leeuwis, A. E., Koene, T., Scheltens, P., Barkhof, F., et al. (2015). White matter hyperintensities relate to clinical progression in subjective cognitive decline. *Stroke*, *46*(9), 2661–2664. doi:10.1161/STROKEAHA.115.009475.
- Bracco, L., Campani, D., Baratti, E., Lippi, A., Inzitari, D., Pracucci, G., et al. (1993). Relation between MRI features and dementia in cerebrovascular disease patients with leukoariosis: a longitudinal study. *Journal of the Neurological Sciences*, *120*(2), 131–136.
- Chimowitz, M. I., Estes, M. L., Furlan, A. J., & Awad, I. A. (1992). Further observations on the pathology of subcortical lesions identified on magnetic resonance imaging. *Archives of Neurology*, *49*(7), 747–752.
- Chui, H. C., & Ramirez-Gomez, L. (2015). Clinical and imaging features of mixed Alzheimer and vascular pathologies. *Alzheimer's Research & Therapy*, *7*(1), 21. doi:10.1186/s13195-015-0104-7.
- Chutinet, A., & Rost, N. S. (2014). White matter disease as a biomarker for long-term cerebrovascular disease and dementia. *Current Treatment Options in Cardiovascular Medicine*, *16*(3), 292. doi:10.1007/s11936-013-0292-z.
- Debette, S., & Markus, H. S. (2010). The clinical importance of white matter hyperintensities on brain magnetic resonance imaging: systematic review and meta-analysis. *BMJ*, *341*, c3666. doi:10.1136/bmj.c3666.
- Ehrensperger, M. M., Berres, M., Taylor, K. I., & Monsch, A. U. (2010). Early detection of Alzheimer's disease with a total score of the German CERAD. *Journal of the International Neuropsychological Society*, *16*(5), 910–920. doi:10.1017/S1355617710000822.
- Fazekas, F., Chawluk, J. B., Alavi, A., Hurtig, H. I., & Zimmerman, R. A. (1987). MR signal abnormalities at 1.5 T in Alzheimer's dementia and normal aging. *AJR. American Journal of Roentgenology*, *149*(2), 351–356. doi:10.2214/ajr.149.2.351.
- Fazekas, F., Kleinert, R., Offenbacher, H., Schmidt, R., Kleinert, G., Payer, F., et al. (1993). Pathologic correlates of incidental MRI white matter signal hyperintensities. *Neurology*, *43*(9), 1683–1689.
- Frackowiak, R. S. J., Friston, K. J., Frith, C. D., Dolan, R. J., Price, C. J., Zeki, S., et al. (Eds.) (2004). *Human brain function*. San Diego: Academic Press.
- Galluzzi, S., Lanni, C., Pantoni, L., Filippi, M., & Frisoni, G. B. (2008). White matter lesions in the elderly: pathophysiological hypothesis on the effect on brain plasticity and reserve. *Journal of the Neurological Sciences*, *273*(1–2), 3–9. doi:10.1016/j.jns.2008.06.023.
- Garde, E., Mortensen, E. L., Krabbe, K., Rostrup, E., & Larsson, H. B. (2000). Relation between age-related decline in intelligence and cerebral white-matter hyperintensities in healthy octogenarians: a longitudinal study. *Lancet*, *356*(9230), 628–634. doi:10.1016/S0140-6736(00)02604-0.
- Gouw, A. A., Seewann, A., van der Flier, W. M., Barkhof, F., Rozemuller, A. M., Scheltens, P., et al. (2011). Heterogeneity of small vessel disease: a systematic review of MRI and histopathology correlations. *Journal of Neurology, Neurosurgery, and Psychiatry*, *82*(2), 126–135. doi:10.1136/jnnp.2009.204685.
- Hofheinz, F., Lougovski, A., Zophel, K., Hentschel, M., Steffen, I. G., Apostolova, I., et al. (2014). Increased evidence for the prognostic value of primary tumor asphericity in pretherapeutic FDG PET for risk stratification in patients with head and neck cancer. *European Journal of Nuclear Medicine and Molecular Imaging*. doi:10.1007/s00259-014-2953-x.
- Jokinen, H., Kalska, H., Ylikoski, R., Madureira, S., Verdelho, A., Gouw, A., et al. (2009). MRI-defined subcortical ischemic vascular disease: baseline clinical and neuropsychological findings. The LADIS study. *Cerebrovascular Diseases*, *27*(4), 336–344. doi:10.1159/000202010.
- Kapeller, P., Barber, R., Vermeulen, R. J., Ader, H., Scheltens, P., Freidl, W., et al. (2003). Visual rating of age-related white matter changes on magnetic resonance imaging: scale comparison, interrater agreement, and correlations with quantitative measurements. *Stroke*, *34*(2), 441–445.
- Keihaninejad, S., Heckemann, R. A., Fagiolo, G., Symms, M. R., Hajnal, J. V., Hammers, A., et al. (2010). A robust method to estimate the intracranial volume across MRI field strengths (1.5 T and 3 T). *NeuroImage*, *50*(4), 1427–1437. doi:10.1016/j.neuroimage.2010.01.064.
- Kim, K. W., MacFall, J. R., & Payne, M. E. (2008). Classification of white matter lesions on magnetic resonance imaging in elderly persons. *Biological Psychiatry*, *64*(4), 273–280. doi:10.1016/j.biopsych.2008.03.024.
- Kim, H. J., Im, K., Kwon, H., Lee, J. M., Kim, C., Kim, Y. J., et al. (2015). Clinical effect of white matter network disruption related to amyloid and small vessel disease. *Neurology*, *85*(1), 63–70. doi:10.1212/WNL.0000000000001705.
- Mazerolle, E. L., Wojtowicz, M. A., Omisade, A., & Fisk, J. D. (2013). Intra-individual variability in information processing speed reflects white matter microstructure in multiple sclerosis. *NeuroImage Clin*, *2*, 894–902. doi:10.1016/j.nicl.2013.06.012.
- McKhann, G., Drachman, D., Folstein, M., Katzman, R., Price, D., & Stadlan, E. M. (1984). Clinical diagnosis of Alzheimer's disease: report of the NINCDS-ADRDA work group under the auspices of Department of Health and Human Services Task Force on Alzheimer's disease. *Neurology*, *34*(7), 939–944.
- Morris, J. C., Mohs, R. C., Rogers, H., Fillenbaum, G., & Heyman, A. (1988). Consortium to establish a registry for Alzheimer's disease (CERAD) clinical and neuropsychological assessment of Alzheimer's disease. *Psychopharmacology Bulletin*, *24*(4), 641–652.
- Mortamais, M., Artero, S., & Ritchie, K. (2014). White matter hyperintensities as early and independent predictors of Alzheimer's disease risk. *Journal of Alzheimer's Disease*, *42*(Suppl 4), S393–S400. doi:10.3233/JAD-141473.
- Muhlau, M., Buck, D., Forschner, A., Boucard, C. C., Arsic, M., Schmidt, P., et al. (2013). White-matter lesions drive deep gray-matter atrophy in early multiple sclerosis: support from structural MRI. *Multiple Sclerosis*, *19*(11), 1485–1492. doi:10.1177/1352458513478673.
- Niemantsverdriet, E., Feyen, B. F., Le Bastard, N., Martin, J. J., Goeman, J., De Deyn, P. P., et al. (2015). Overdiagnosing vascular dementia using structural brain imaging for dementia work-up. *Journal of Alzheimer's Disease*, *45*(4), 1039–1043. doi:10.3233/JAD-142103.
- O'Sullivan, M. (2010). Imaging small vessel disease: lesion topography, networks, and cognitive deficits investigated with MRI. *Stroke*, *41*(10 Suppl), S154–S158. doi:10.1161/STROKEAHA.110.595314.
- Pantoni, L., Fierini, F., Poggesi, A., & Group, L. S. (2015). Impact of cerebral white matter changes on functionality in older adults: an overview of the LADIS study results and future directions. *Geriatrics & Gerontology International*, *15*(Suppl 1), 10–16. doi:10.1111/ggi.12665.
- Prins, N. D., van Straaten, E. C., van Dijk, E. J., Simoni, M., van Schijndel, R. A., Vrooman, H. A., et al. (2004). Measuring progression of cerebral white matter lesions on MRI: visual rating and volumetrics. *Neurology*, *62*(9), 1533–1539.
- Reitan, R. M. (1958). Validity of the trail making test as an indicator of organic brain damage. *Perceptual and Motor Skills*, *8*, 271–276.

- Roman, G. C., Tatemichi, T. K., Erkinjuntti, T., Cummings, J. L., Masdeu, J. C., Garcia, J. A., et al. (1993). Vascular dementia: diagnostic criteria for research studies. Report of the NINDS-AIREN International Workshop. *Neurology*, *43*, 250–260.
- Sabri, O., Ringelstein, E. B., Hellwig, D., Schneider, R., Schreckenberger, M., Kaiser, H. J., et al. (1999). Neuropsychological impairment correlates with hypoperfusion and hypometabolism but not with severity of white matter lesions on MRI in patients with cerebral microangiopathy. *Stroke*, *30*(3), 556–566.
- Salthouse, T. A. (2011). What cognitive abilities are involved in trail-making performance? *Intelligence*, *39*(4), 222–232. doi:10.1016/j.intell.2011.03.001.
- Scarpelli, M., Salvolini, U., Diamanti, L., Montironi, R., Chiaromoni, L., & Maricotti, M. (1994). MRI and pathological examination of post-mortem brains: the problem of white matter high signal areas. *Neuroradiology*, *36*(5), 393–398.
- Scheltens, P., Barkhof, F., Leys, D., Pruvo, J. P., Nauta, J. J., Vermersch, P., et al. (1993). A semiquantitative rating scale for the assessment of signal hyperintensities on magnetic resonance imaging. *Journal of the Neurological Sciences*, *114*(1), 7–12.
- Schmidt, R., Schmidt, H., Kapeller, P., Lechner, A., & Fazekas, F. (2002). Evolution of white matter lesions. *Cerebrovascular Diseases*, *13*(Suppl 2), 16–20.
- Schmidt, P., Gaser, C., Arsic, M., Buck, D., Forschler, A., Berthele, A., et al. (2012). An automated tool for detection of FLAIR-hyperintense white-matter lesions in multiple sclerosis. *NeuroImage*, *59*(4), 3774–3783. doi:10.1016/j.neuroimage.2011.11.032.
- Shirk, S. D., Mitchell, M. B., Shaughnessy, L. W., Sherman, J. C., Locascio, J. J., Weintraub, S., et al. (2011). A web-based normative calculator for the uniform data set (UDS) neuropsychological test battery. *Alzheimer's Research & Therapy*, *3*(6), 32. doi:10.1186/alzrt94.
- Soriano-Raya, J. J., Miralbell, J., Lopez-Cancio, E., Bargallo, N., Arenillas, J. F., Barrios, M., et al. (2012). Deep versus periventricular white matter lesions and cognitive function in a community sample of middle-aged participants. *Journal of the International Neuropsychological Society*, *18*(5), 874–885. doi:10.1017/S1355617712000677.
- Sun, J., Yu, X., Jiaerken, Y., Song, R., Huang, P., Wang, C., et al. (2016). The relationship between microvasculature in white matter hyperintensities and cognitive function. *Brain Imaging and Behavior*. doi:10.1007/s11682-016-9531-8.
- Tate, D. F., Jefferson, A. L., Brickman, A. M., Hoth, K. F., Gunstad, J., Bramley, K., et al. (2008). Regional white matter signal abnormalities and cognitive correlates among geriatric patients with treated cardiovascular disease. *Brain Imaging and Behavior*, *2*(3), 200–206. doi:10.1007/s11682-008-9032-5.
- Valverde, S., Oliver, A., Roura, E., Pareto, D., Vilanova, J. C., Ramio-Torrenta, L., et al. (2015). Quantifying brain tissue volume in multiple sclerosis with automated lesion segmentation and filling. *NeuroImage Clinical*, *9*, 640–647. doi:10.1016/j.nicl.2015.10.012.
- van den Heuvel, D. M., ten Dam, V. H., de Craen, A. J., Admiraal-Behloul, F., van Es, A. C., Palm, W. M., et al. (2006). Measuring longitudinal white matter changes: comparison of a visual rating scale with a volumetric measurement. *AJNR. American Journal of Neuroradiology*, *27*(4), 875–878.
- Wadell, H. (1935). Volume, shape, and roundness of quartz particles. *Journal of Geology*, *43*(3), 250–280.
- Wahlund, L. O., Barkhof, F., Fazekas, F., Bronge, L., Augustin, M., Sjogren, M., et al. (2001). A new rating scale for age-related white matter changes applicable to MRI and CT. *Stroke*, *32*(6), 1318–1322.
- Weintraub, S., Salmon, D., Mercaldo, N., Ferris, S., Graff-Radford, N. R., Chui, H., et al. (2009). The Alzheimer's disease centers' uniform data set (UDS): the neuropsychologic test battery. *Alzheimer Disease and Associated Disorders*, *23*(2), 91–101. doi:10.1097/WAD.0b013e318191c7dd.
- Ye, B. S., Seo, S. W., Kim, J. H., Kim, G. H., Cho, H., Noh, Y., et al. (2015). Effects of amyloid and vascular markers on cognitive decline in subcortical vascular dementia. *Neurology*, *85*(19), 1687–1693. doi:10.1212/WNL.0000000000002097.
- Youden, W. J. (1950). Index for rating diagnostic tests. *Cancer*, *3*(1), 32–35.